Sensors-Embedded Cutting Tools to Accelerate Digital Transformation in Cutting Processes

Yusuke KURIYAMA*, Koji KOSAI, Masashi HARADA,
Yusuke KOIKE, Kota YOSHIDA, and Daisuke MURAKAMI

During cutting processes, cutting edges cannot be directly observed, leading to reliance on skilled workers' intuition and experience for optimizing cutting conditions. In recent years, sensors equipped in machine tools have been utilized to comprehensively monitor machining conditions including cutting forces. However, their sensitivity and accuracy are insufficient due to distance between the cutting point and measurement position. To address this challenge, we have developed "Sumi Force," a sensing tool that measures cutting forces in real-time by embedding strain sensors in the tool holder, where inserts, drills, or end mills are held, closest to the cutting point. The measured data is wirelessly transmitted outside the machine tool, enabling easy integration to various machines and production lines used by customers. This paper introduces a new solution service that utilizes "Sumi Force" to optimize machining processes for customers, and discusses the development of techniques to detect anomalies such as tool wear and breakage based on changes in cutting force.

Keywords: cutting, process monitoring, sensor, cutting force, anomaly detection

1. Introduction

Cutting points cannot be directly observed due to chips and cutting fluid discharged during the processes. For this reason, optimization of machining conditions and confirmation of chipping have been largely dependent on the operator's senses. In recent years, however, the shortage of skilled operators has led to the development of technologies that monitor machining conditions on behalf of the operator. For example, technologies to visualize comprehensive machining conditions such as cutting force based on machine tool spindle currents and drive system motor currents have been put to practical use.[(1)–(3)] However, the sensitivity and accuracy of these technologies are not sufficient because the measurement points are far from the cutting points.

In response, we have developed a sensing tool "Sumi Force," sensors-embedded cutting tool. "Sumi Force" can measure cutting force during machining by embedding strain sensors in the holder that holds the insert, drill, or end mill closest to the cutting point. The data is wirelessly transmitted outside the machine tool. By mounting the sensors in the holder close to the cutting edge, the machining process can be monitored with high sensitivity and accuracy.[(4),(5)]

The sensing tool "Sumi Force" can be easily integrated into a machine tool, making it possible to measure cutting force on the customer's actual machine and production line. We are developing Digital Analysis Support to determine the cause of problems and optimize machining conditions. The sensing tool can also detect tool wear and chipping based on changes in cutting force. This report describes the development of machining condition optimization at a customer using the sensing tool, tool wear estimation, and anomaly detection technologies.

2. Optimization of Machining Conditions with Digital Analysis Support

2-1 Outline of the sensing tool for turning

Figure 1 shows an overview of the sensing tool developed for turning. Strains sensors are embedded in the bottom and back of the sensing tool for turning, as well as a wireless communication and control board on the front. The sensing tool has the same size and specifications as the normal holder. Due to the characteristic, by replacing the current holder with the sensing tool and attaching the receiver to a window of the machine tool, changes in cutting force during machining can be easily measured. The measured quantities are not three-component forces (principal, feed, and thrust force), but two-component forces applied vertically and horizontally to the holder. As shown in Fig. 2, the strain sensor embedded in the bottom mainly detects the bending strain due to the principal force as a composite value with the bending and compressive

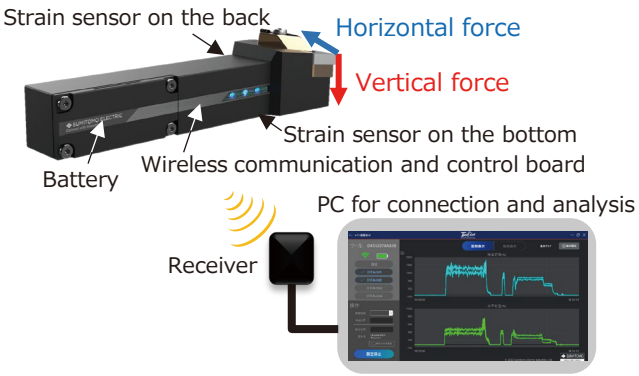

Fig. 1. Overview of the sensing tool for turning

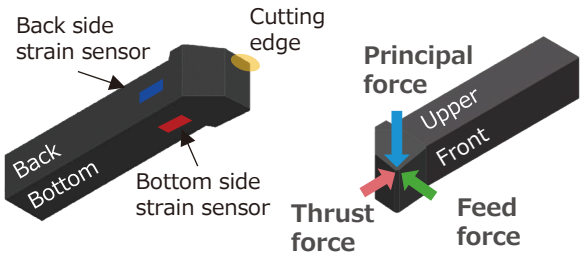

Fig. 2. Relationship between sensor position and three-component forces

strains due to the thrust force. Finally, it is outputted as the vertical force calibrated by applying a load vertically to the holder. Similarly, the strain sensor embedded in the back mainly detects the bending strain due to the feed force as a composite value with the bending and compressive strains due to the thrust force, which is outputted as the horizontal force calibrated by applying a load horizontally to the holder.

The sampling frequency is approximately 2 kHz, and Bluetooth LE*[1] is used for wireless communication. Although the holder is carved for embedding components including sensors, when machined with normal protrusion, the stiffness is 99% of that of a normal holder.

2-2 Digital analysis support using the sensing tool

Figure 3 shows an example using a sensing tool in an actual production line of a customer manufacturing automotive parts. As shown in the figure, the cutting force can be easily measured by equipping the sensing tool on the turret in the machining chamber of the lathe as well as the receiver on the window outside the lathe.

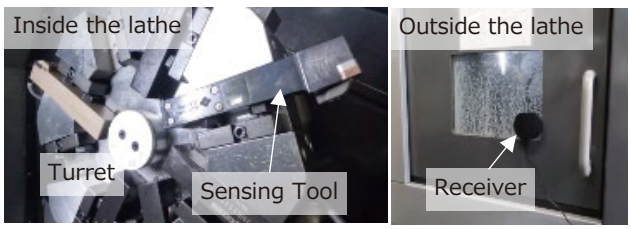

Fig. 3. Sensing tool integrated into an actual production line

Figure 4 shows the tool path and measured cutting forces. In Path 1, the cutting forces remains stable due to a constant depth of cut, and then rapidly increases at the point where the tool contacts the wall section A in the figure. This sudden increase in cutting forces is one of the major causes of chipping. The sensing tool quantitatively reveals that at the point, the vertical force is 1.3 times higher and the horizontal force is 2 times higher in the customer's actual production line. In addition, in Path 3, the cutting forces changes in accordance with the variation of the depth of cut, indicating that the sensing tool is able to visualize the machining state well. In this case, the feed rate was reduced to prevent chipping in section A, where the cutting forces rapidly increases. This allows to select a tool grade that focuses more on wear resistance to extend tool life.

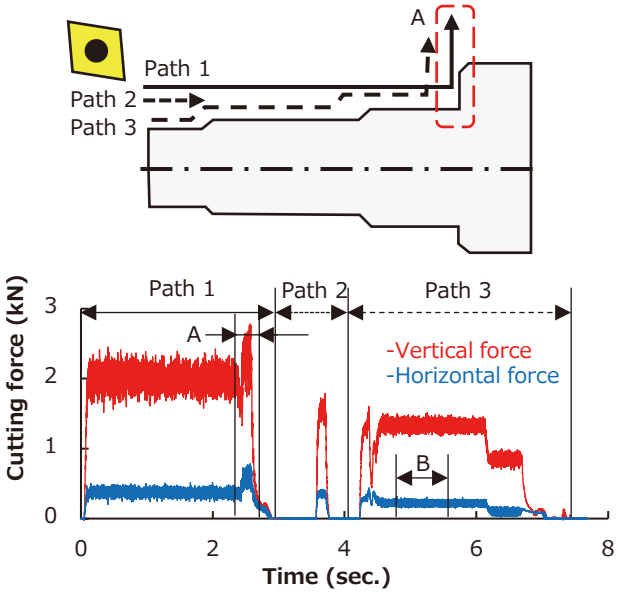

Fig. 4. Change in tool path and cutting forces

Figure 5 shows change in the average horizontal force in section B of Path 3 with respect to quantity of machined workpiece. It can be seen that the cutting increases due to tool wear as the machining workpieces quantity increases. Furthermore, slope of the increase in cutting force for the proposed new tool grade is smaller than that for the conventional grade, indicating that wear resistance is improved.

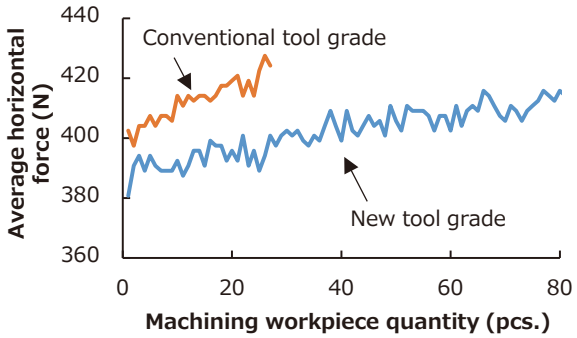

Fig. 5. Change in the average horizontal force with respect to machining workpiece quantity

In this case, we introduced a countermeasure against a rapid increase in cutting force. In addition, it is also possible to detect chip biting, in which extended chips bitten between the cutting edge and workpiece, as well as abnormal vibration during machining, called chattering. Therefore, the sensing tool is useful for quantitatively

optimizing machining conditions on the customer's actual production line.

3. Tool Wear Monitoring on a Small Lathe

3-1 Outline of the sensing tool for small lathes

Figure 6 shows a sensing tool for small lathes. The space in a small lathe is limited. In addition, carving the holder to embed the sensor greatly reduces the holder's stiffness due to its thin body. Therefore, the sensing tool for small lathes, which are used with a gang type tool rest, is equipped with the sensor and wireless communication and control board on back of the holder. This structure enables measurement of change in the horizontal force applied to the cutting edge. In this paper, we examined whether the tool could detect wear propagation.

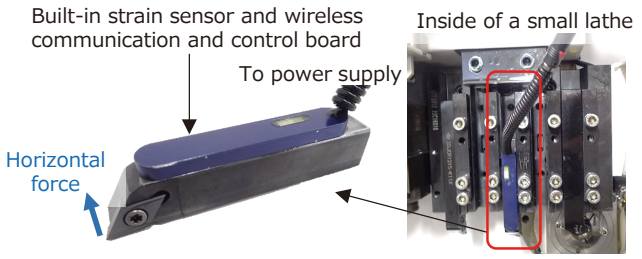

Fig. 6. Overview of the sensing tool for small lathes

3-2 Results of monitoring tool edge wear by amount of strain

Table 1 shows the experimental conditions. The experiment was performed on a small spindle-moving lathe. A cycle of 14 mm length cutting in two paths and a part-off process was repeated. Two tool grades, cermet (P10) and coated carbide (P40-PVD), were used to investigate the correlation between tool wear and the horizontal force measured by the sensing tool. In this study, the amount of strain was substituted as the horizontal force.

Table 1. Experimental conditions

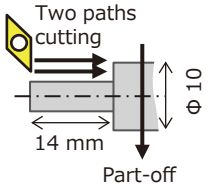	Tool: DCGT11T302R-FX Cermet (P10) Coated carbide (P40-PVD) Workpiece material: X2CrNiMo17-12-2 Cutting speed: V_c = 120 m/min Feed: f = 0.05mm/rev. Depth of cut: a_p= 1.0 mm Cutting length: l = 14 mm/path Atmosphere: Wet, insoluble

Figure 7 is an example of the waveform of the amount of strain on the holder during the two paths cutting. The measured strain is compressive one and negative, but is represented as a positive absolute value. The amount of strain associated with cutting force increases immediately after the beginning of cutting and then becomes almost constant. It is also observed that the cutting force increased unstably and rapidly near the end of the second path. This may be due to chip biting.

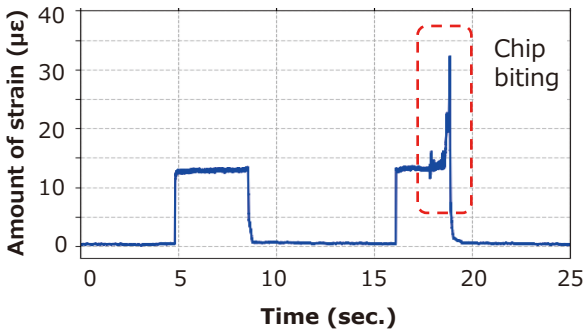

Fig. 7. Strain measurement result

Figure 8 shows change in the holder's strain and flank wear width. As shown in the figure, they exhibit good correspondence and the correlation coefficient exceeds 0.98 for both inserts. In addition, when comparing cermet and coated carbide, both the tool wear and the amount of strain are smaller for coated carbide. Hence, difference in wear propagation speed between the different inserts is also visualized.

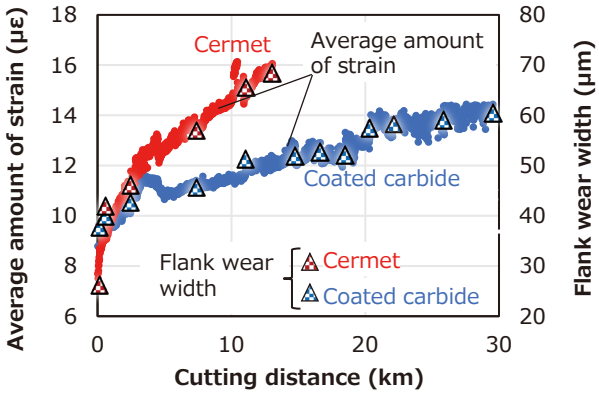

Fig. 8. Change in average amount of strain and flank wear

The above results demonstrate that wear propagation can be monitored even in a small lathe by utilizing the sensing tool.

4. Cutting Edge Conditions Monitoring during End Milling

4-1 Outline of the sensing tool for milling and drilling

Figure 9 shows the sensing tool for milling and drilling. The sensing tool measures the four components M_x, M_y, M_z and F_z by converting the strain measured on the tool holder caused by cutting force. In this paper, for easy

understanding of the cutting force direction at the cutting edge, the moment loads M_x and M_y are redefined as M'_x and M'_y. M'_x and M'_y possess axes and directions which coincide with those of cutting forces bending the tool holder, as shown in Fig. 9.

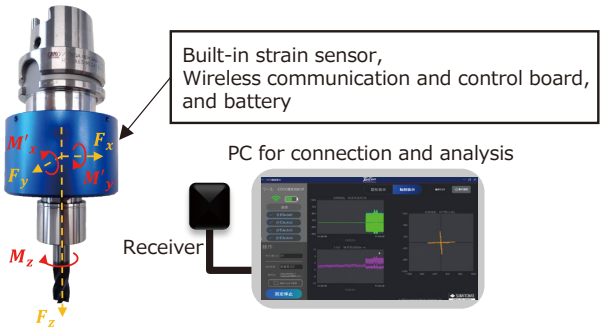

Fig. 9. Overview of the sensing tool for milling and drilling

In the sensing tool, the sensor and tool rotate as one unit, allowing measurement in the rotational coordinate system of the cutting tool. When the cutting force is assumed to act only at the cutting edge, the cutting forces F'_x and F'_y can be calculated by dividing the measured moment loads M'_x and M'_y by the distance between the sensor and tool tip, namely, the length of the moment load arm. By plotting F'_x and F'_y, a graph showing a characteristic geometric shape corresponding to change in cutting force on a plane perpendicular to the tool rotation axis can be obtained, as shown in Fig. 10. It should be mentioned that F'_x and F'_y exhibit the same geometric shape of the graph as M'_x and M'_y since they are proportional. This geometry is hereinafter referred to as the "graph geometry". In the graph, cutting force during steady-state machining is plotted in the XY plane. The cutting force is measured over a time width of one tool revolution or more. Since this graph geometry changes depending on the cutting edge conditions, the geometry might be useful for detecting anomalies such as tool wear and chipping. In this paper, it is attempted to monitor wear propagation based on change in similarity between the graph geometry measured by the sensing tool and the theoretical one under normal conditions.

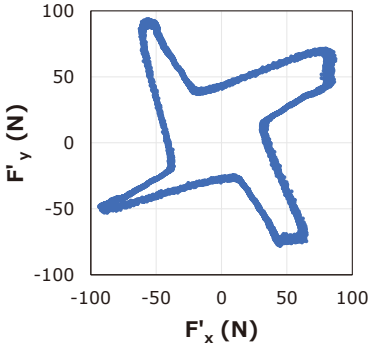

Fig. 10. Cutting force XY graph

4-2 Estimation of the geometry using on instantaneous cutting force model

In order to obtain the theoretical graph geometry under normal conditions, an instantaneous cutting force model is modified.[6],[7] In the modified model, the cutting cross-sectional area is calculated where each cutting edge contacts the workpiece during the cutting process. In this model, as shown in Fig. 11, the end mill is divided into minute disk elements on the plane perpendicular to the tool axis. It is assumed that a micro-cutting force acts on any cutting edge i in each minute disk element at a given instant. In the model, moment load is calculated in the cutting tool rotation coordinate system where the origin locates at the sensor in the holder. The model is simplified for calculating moment load without specific cutting force. In addition, the radial position variation of each cutting edge is statically measured and considered as change in underformed chip thickness.

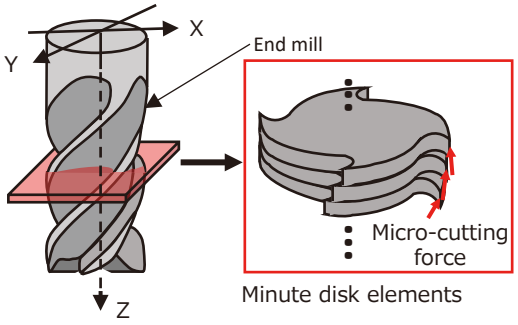

Fig. 11. Concept of the instantaneous cutting force model

In the model with the above modifications, the moment load vector $\boldsymbol{M'_{tool}}$ acting on the cutting tool is calculated as the sum of the moment load vectors $\boldsymbol{M'_i}$ acting on the entire part of any cutting edge i, by using the following formula.

$$\boldsymbol{M'_{tool}} = \sum_{i=1}^{N} \boldsymbol{M'_i}$$

$$= \sum_{i=1}^{N} \left\{ \int_{L-a_p}^{L} z\boldsymbol{R_i}(z) K_c \boldsymbol{E} \cdot (h_i(z) + r_i) dz \right\} \quad \cdots\cdots (1)$$

N is the number of cutting edges, L is the axial distance between the strain sensor and tool tip, a_p is the axial depth of cut, z is the axial distance between the strain sensor and minute disk element, $\boldsymbol{R_i}(z)$ is a rotation matrix showing change in phase of the cutting edge i with helix angle and cutting edge position, K_c is a scalar value indicating the specific cutting force at the cutting edge, $\boldsymbol{E}$ is a vector in the direction of the cutting force at the cutting edge, $h_i(z)$ is radial undeformed chip thickness calculated geometrically ignoring radial edge position variation, and r_i is change in undeformed chip thickness due to radial edge position variation. If a_p is in a small range, it can be approximated that z ≈ L, and Eq. (1) can be simplified as follows.

$$\boldsymbol{M'_{tool}} = LK_c \sum_{i=1}^{N} \left\{ \int_{L-a_p}^{L} \boldsymbol{R_i}(z)\boldsymbol{E} \cdot (h_i(z) + r_i) dz \right\}$$
$$= LK_c \sum_{i=1}^{N} \boldsymbol{A_i} = LK_c \boldsymbol{A_{tool}} \quad \cdots\cdots\cdots\cdots\cdots (2)$$

$\boldsymbol{A_i}$ is defined as the cutting cross section vector with the size of the cutting cross section. The above equation derives $\boldsymbol{A_{tool}}$ as the sum of the cutting cross section vectors at each cutting edge. When a_p is in a small range, $\boldsymbol{A_{tool}}$ exhibits the same graph geometry as $\boldsymbol{M'_{tool}}$ and can be calculated without using the specific cutting force K_c. In addition, the cutting forces F'_x and F'_y measured by the sensing tool also exhibit the same graph geometry as moment loads. Hence, the estimated graph of $\boldsymbol{A_{tool}}$ was used as the theoretical graph under normal conditions and compared with the graph measured by the sensing tool.

4-3 Results of monitoring tool wear by graph geometry

A tool life test of an end mill was performed under the conditions in Table 2 for attempting to monitor tool wear. The monitoring was based on change in similarity between the estimated graph geometry of $\boldsymbol{A_{tool}}$ and the measured one of the moment loads measured by the sensing tool. The similarity was quantitatively evaluated by image processing technique shown in Fig. 12. First, in each graph, the size of the graph was aligned based on the maximum value. Then, the geometric shape was extracted, and the graph was converted to a binary image. The region closed by the geometric shape was set to 1, and the other region was set to 0, which were expressed in white and black, respectively. The estimated or measured image was overlaid with the other one. Afterward, the area of the white region, which indicates the region of exclusive-or where 1 and 0 do not match, was calculated. The smaller area of this white region indicates the higher similarity between the two images.

Table 2. Experimental conditions

Tool: GSX4120C-2D (Sumitomo Electric Hardmetal Corp.) Φ 12, 4 flutes, torsion angle 30°, equal pitch
Protrusion: 35 mm
Workpiece material: C50
Cutting speed Vc = 80 m/min
Feed f = 0.02 mm/tooth
Axial depth of cut a_p = 1.0 mm
Radial depth of cut a_e = 0.362 mm
Cutting distance L = 30 m (0.15 m per one path × 200 pathes)
Cutting direction: Down-cut
Atmosphere: Dry

Figure 13 shows the flank faces observed after 20 or 200 paths of machining, as well as the estimated $\boldsymbol{A_{tool}}$ graphs, the measured moment load graphs, and the images of exclusive-or. The values in the measurement graphs are the amounts of radial edge position variation at each cutting edge with using the edge marked with * as a reference. It can be seen that as the flank wear width increases, the width of the lines corresponding to each edge in the measurement graph widens between the center of each cross line and that of the graph. This change is presumably due to the increase in the radial force with wear propagation.

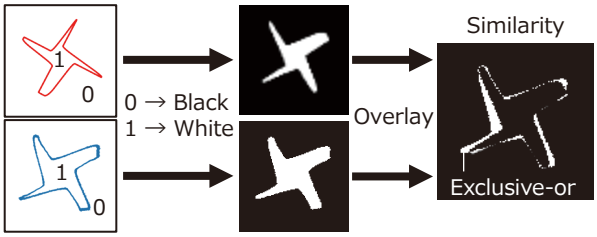

Fig. 12. Calculation of similarity by exclusive-or

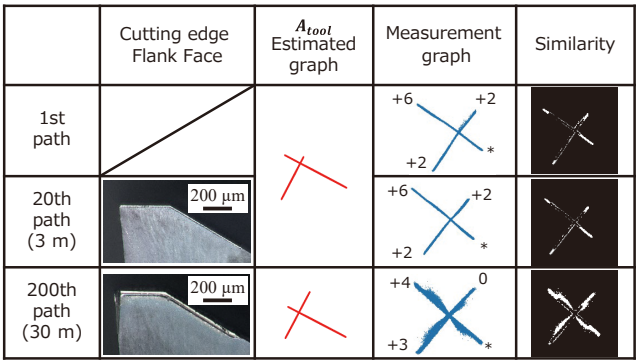

Fig. 13. Estimated/measured graphs and similarity

Figure 14 shows the flank wear width and the area of the exclusive-or region measured at each cutting distance of 3 m (20 paths). For comparison, the maximum moment load and the maximum torque around the rotation axis during steady-state machining were also measured. All the values except the flank wear width were divided by the value of the first path for nomalization. Figure 14 indicates that differently from the maximum values of moment load and torque, the area of the exclusive-or region gradually increases after the cutting distance of 9 m, with a slight spike at 30 m. The trend coincides with that of the flank wear width. This fact demonstrates effectiveness of the method based on the geometric similarity between the estimated and measured graphs for monitoring cutting edge conditions.

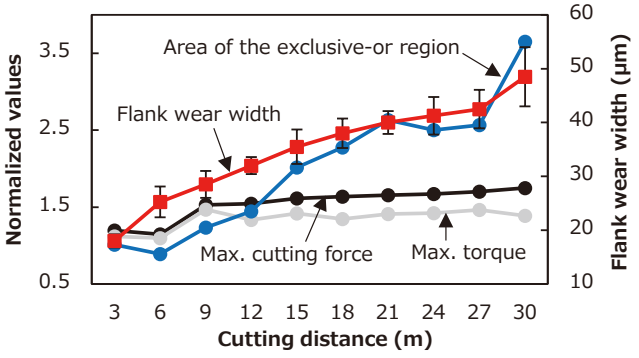

Fig. 14. Variation in the flank wear width and measured values

5. Conclusion

This paper introduces sensors-embedded tool holders, the sensing tool “Sumi Force”, as well as their applications. “Sumi Force” enables to monitor machining conditions sensitively and precisely by embedding sensors in the holder near the cutting point. It has been demonstrated that due to the characteristic, “Sumi Force” can be widely used as an anomaly detection technology to improve machining conditions on customers’ actual production lines, as well as to monitor tool wear in small lathes and end mill machining. In the future, we will further develop this technology and realize automated machining, reduction of losses, and reduction of power consumption through highly efficient machining for wide contribution to society.

Technical Term

∗1 Bluetooth LE (Low energy): A type of Bluetooth used for low-power, short-range wireless communications between PCs and IoT devices. It can send and receive data within a certain communication range while reducing battery consumption.
“Bluetooth” and “Bluetooth Low Energy” are trademarks or registered trademarks of Bluetooth SIG, INC. in the United States and other countries.

References

(1) S. Bombiński, K. Błażejak, M. Nejman and K. Jemielniak, “Sensor signal segmentation for tool condition monitoring,” Procedia CIRP, vol. 46, pp. 155-160 (2016)
(2) R. Sato, M. Hasegawa and K. Shirase,“ Cutting Force Monitoring based on the Frequency Analysis of Feed Motor Torques,” Journal of SME Japan, vol.2, pp. 7-12 (2013)
(3) T. Watanabe, I. Kono and H. Onozuka, “Anomaly detection methods in turning based on motor data analysis,” Procedia Manufacturing, vol. 48, pp. 882-893 (2020)
(4) H. Shizuka, K. Sakai, K. Honda, R. Okada, and K. Miyajima, “In-situ tool wear monitoring using semiconductor strain sensor in diamond cutting,” euspen’s 20th International Conference & Exhibition (2020)
(5) M. Z. Asadzadeh, A. Eiböck, H.-P. Gänser, T. Klünsner, M. Mücke, L. Hanna, T. Teppernegg, M. Treichler, P. Peissl and C. Czettl, “Tool damage state condition monitoring in milling processes based on the mechanistic model goodness-of-fit metrics,” Journal of Manufacturing Processes, vol. 80, pp. 612-623 (2022)
(6) J. W. Sutherland and R. E. DeVor, “An Improved Method for Cutting Force and Surface Error Prediction in Flexible End Milling Systems,” Journal of Engineering for Industry, vol. 108, pp. 269-279 (1986)
(7) K. Kaneko, I. Nishida, R. Sato and K. Shirase.” Instantaneous rigid force model based on oblique cutting to predict milling force,” The Japan Society of Mechanical Engineers, vol.83, no.856 (2017)

Contributors The lead author is indicated by an asterisk (∗).

Y. KURIYAMA*
• Assistant Manager, Advanced Materials Laboratory

K. KOSAI
• Advanced Materials Laboratory
Doctor of Engineering

M. HARADA
• Advanced Materials Laboratory

Y. KOIKE
• Group Manager, Sumitomo Electric Hardmetal Corp.
Doctor of Engineering

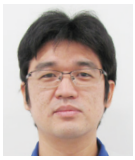

K. YOSHIDA
• Sumitomo Electric Hardmetal Corp.

D. MURAKAMI
• Fellow
Advanced Materials Laboratory
Doctor of Engineering